

Epipolar Geometry of Line Cameras Moving with Constant Velocity and Attitude

Ayman F. Habib, Michel F. Morgan, Soo Jeong, and Kyung-Ok Kim

Image resampling according to epipolar geometry is an important prerequisite for a variety of photogrammetric tasks. Established procedures for resampling frame images according to epipolar geometry are not suitable for scenes captured by line cameras. In this paper, the mathematical model describing epipolar lines in scenes captured by line cameras moving with constant velocity and attitude is established and analyzed. The choice of this trajectory is motivated by the fact that many line cameras can be assumed to follow such a flight path during the short duration of a scene capture (especially when considering space-borne imaging platforms). Experimental results from synthetic along-track and across-track stereo-scenes are presented. For these scenes, the deviations of the resulting epipolar lines from straightness, as the camera's angular field of view decreases, are quantified and presented.

Keywords: Epipolar geometry, epipolar lines, normalized images, line cameras, along-track stereo coverage, across-track stereo coverage.

I. Introduction

Line cameras have been introduced for their potential in capturing high-resolution imagery, which can be used for ortho-photo generation and updating spatial databases [1]. Space-borne line cameras with up to one-meter resolution from commercial satellites could bring more benefits and challenges to traditional topographic mapping using aerial images [2]. For example, epipolar resampling of images captured by a frame camera is an established process, which is readily available in current photogrammetric workstations [3]. On the other hand, resampling scenes captured by line cameras according to epipolar geometry is not a trivial task. The difficulty of resampling these scenes can be to a certain degree attributed to the complicated nature of the perspective geometry of line cameras and the shape of the resulting epipolar lines.

Kim [4] investigated the epipolar geometry of scenes captured by line cameras moving in a trajectory, where the position and heading components are described by second-order polynomial functions, while the roll and pitch angles are represented by first-order polynomials. The author concluded that the epipolar lines in scenes captured from such a trajectory are not straight lines. The fact that the resulting epipolar lines are not straight makes the normalized image generation of such scenes extremely difficult if not impossible. This is due to the fact that normalized image generation aims at transforming the original scenes in such a way that the epipolar lines coincide with the rows or columns of the output imagery [5].

In this paper, the epipolar geometry associated with scenes captured by line cameras from a system traveling with constant velocity and attitude along its trajectory is analyzed. Such a trajectory is investigated for two reasons. First, we would like to investigate if such a trajectory would lead to straight epipolar

Manuscript received June 25, 2004; revised Jan. 5, 2005.

Ayman F. Habib (phone: +1 403 220 7105, email: habib@geomatics.ucalgary.ca) and Michel F. Morgan (email: mfmorgan@ucalgary.ca) are with Department of Geomatics Engineering, University of Calgary, Canada.

Soo Jeong (email: soo@andong.ac.kr) is with Department of Civil Engineering, Andong National University, Andong, Korea.

Kyung-Ok Kim (email: kokim@etri.re.kr) is with Telematics & USN Research Division, ETRI, Daejeon, Korea.

lines. Second, it closely resembles the flight path of the onboard space-borne platforms of imaging systems. The next two sections contain background information regarding the epipolar geometry of frame images and the imaging geometry of line cameras. These are followed by a comprehensive analysis of the epipolar geometry of scenes captured by imaging systems moving with a constant velocity and attitude. Finally, experimental results from synthetic data, conclusions, and recommendations for future work are presented.

II. Epipolar Geometry of Frame Cameras: Background

Before going into the details of the epipolar geometry associated with line cameras, let us start by a brief review of the epipolar geometry of imagery captured by frame cameras. Figure 1 shows two frame images that have been relatively oriented (i.e., the relative relationship between their image coordinate systems is similar to that at the time of exposure). The symbols O and O' are the perspective centers of the left and right images at the time of exposure, respectively. Following are some definitions, pertinent to epipolar geometry [3].

Epipolar plane: The epipolar plane for a given image point p in one of the images is the plane that passes through that point and the perspective centers, O and O' .

Epipolar line: The epipolar line can be defined in two ways. It can be defined as the intersection of the epipolar plane with the image/focal plane. Such an intersection produces a straight line. Alternatively, the epipolar line in the right image can be represented by the locus of all possible conjugate points to a selected point in the left image. Such a locus can be derived by changing the height of the corresponding object

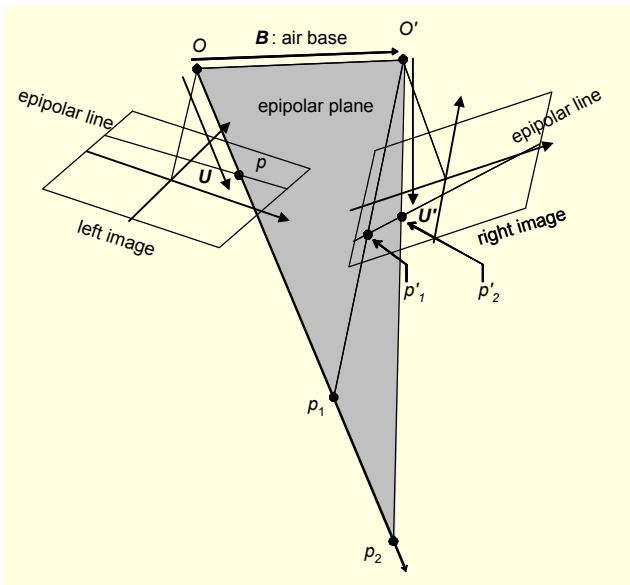


Fig. 1. Epipolar geometry of relatively oriented frame images.

point along the light ray connecting the perspective center and the image point under consideration, shown in Fig. 1. It should be noted that no digital elevation model is needed to determine the epipolar line.

The coplanarity condition [6] can be used to determine the equation of the epipolar line. The underlying concept of the coplanarity condition is that the following vectors, shown in Fig. 1, are coplanar:

- The air base vector connecting the two perspective centers (B);
- The vector connecting the point of interest p in the left image with its perspective center (U); and
- The vector connecting the corresponding point in the right image with its perspective center (U').

The coplanarity condition can be expressed by the determinant or the triple product in (1).

$$\begin{vmatrix} B^T \\ U^T \\ U'^T \end{vmatrix} = \begin{vmatrix} (B_x, B_y, B_z) \\ [R_{(\omega, \phi, \kappa)} (x_p, y_p, -c)^T] \\ [R_{(\omega', \phi', \kappa')} (x'_{p'}, y'_{p'}, -c)^T] \end{vmatrix} = (U \times U') \cdot B = 0, \quad (1)$$

where B_x, B_y, B_z are the components of the air base vector B with respect to the object coordinate system; $R_{(\omega, \phi, \kappa)}$ is the rotation matrix associated with the left image coordinate system; $R_{(\omega', \phi', \kappa')}$ is the rotation matrix associated with the right image coordinate system; x_p, y_p are the coordinates of point p in the left image; $x'_{p'}, y'_{p'}$ are the coordinates of the corresponding point in the right image; and c is the camera's principal distance.

One should note that the three vectors in (1) should refer to the same coordinate system (i.e., the ground coordinate system). Given the left image point coordinates, the interior orientation parameters, and the relative orientation parameters, the only unknowns in (1) would be the coordinates of the corresponding right image point ($x'_{p'}, y'_{p'}$). Expanding the determinant (or the triple product) in (1) will lead to a linear equation in ($x'_{p'}, y'_{p'}$), which is the equation of the epipolar line in the right image.

III. Line Cameras: Imaging Methodology and Stereo-Coverage Scenarios

Before discussing the technical details of the epipolar geometry of line cameras, we will briefly present some background related to line cameras. The next subsection explains the imaging methodology of line cameras and how it is different from that associated with traditional frame cameras. This will be followed by an explanation of various options of

stereo-coverage using line cameras.

1. Imaging Methodology

Digital frame cameras capture the image data using a two-dimensional CCD array in the focal plane. The limited number of pixels in current digital imaging systems will not allow for the capture of digital frame imagery with geometric resolution and ground coverage similar to those of analog frame imagery. Line cameras can be used to obtain large ground coverage and maintain a ground resolution comparable with scanned analog photographs. These cameras capture a one-dimensional image (narrow strip) per snapshot. Successive coverage of contiguous areas on the object space is achieved by moving the line camera (airborne or space-borne) along its trajectory while having an open shutter. Such an imaging scenario would yield a sequence of one-dimensional images. The final scene over an area of interest is obtained by stitching together the resulting one-dimensional images. It is important to note that every image is associated with one exposure station, and therefore each image has its own set of exterior orientation parameters. In this paper, a clear distinction is made between the two terms, *scene* and *image* [7]. An *image* is defined as the recorded sensory data associated with one exposure station. In the case of a frame image, the recorded data is captured from one exposure station, and consequently it constitutes a complete image. In the case of a line camera, there are many one-dimensional images. Each image has its own exposure station. On the other hand, a *scene* is defined as the recorded sensory data associated with one (as in frame images) or more exposure stations (as in line cameras) that maps a two-dimensional area in the object space in a short time period. According to the previous definitions, an image and a scene are identical terms when dealing with imagery captured by frame cameras. On the other hand, a scene is a collection of consecutive one-dimensional images captured by a line camera.

Consequently, it is important to distinguish between scene and image coordinates when dealing with imagery captured by line cameras. As shown in Fig. 2(b), i and y are the scene coordinates, while in Fig. 2(a), x_i and y_i are the image coordinates within image number i . It is important to note that d in Fig. 2(a) is the distance of the linear array from the principal point. Since the linear array has a width of one pixel and no sub-pixel accuracy is considered along that direction, we have $x_i = d$, which can be zero or very close to zero for the cases of IKONOS, SPOT, and the nadir-looking linear array of a three-line camera. For the forward and backward looking linear arrays in three-line cameras, d is different from zero. To maintain a height-base ratio of one, this distance is usually chosen to be half the principal distance.

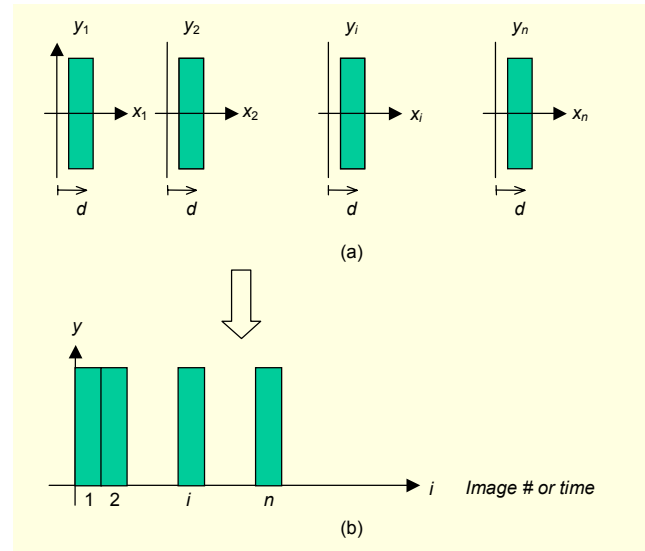


Fig. 2. (a) A sequence of 1D images (b) constituting a scene.

2. Stereo Coverage Scenarios

One of the main objectives of photogrammetry is to derive three-dimensional coordinates from two-dimensional images/scenes. This objective is achieved by intersecting conjugate light rays associated with corresponding points in overlapping views. Therefore, the availability of different views or stereo coverage of the area of interest is essential for deriving three-dimensional coordinates from two-dimensional imagery. In line cameras, stereo coverage can be achieved using one of the following scenarios.

- *One linear array and across-track stereo coverage using roll angles:* Stereo coverage can be achieved by tilting the camera sideways across the flight direction (different roll angles), as shown in Fig. 3(a). This technique has been adopted in SPOT and KOMPSAT-1. A drawback of such stereo-coverage is the large time gap between scenes constituting the stereo pair. Consequently, changes in the object space and/or imaging conditions might be expected between the stereo-scenes [1], [8].

- *One linear array and along-track stereo coverage using pitch angles:* In this case, the camera is tilted forward and backward along the flight direction (different pitch angles), as Fig. 3(b) shows. This type of stereo coverage is used in IKONOS [9]. This method has the advantage of reducing the time gap between the scenes constituting the stereo pair.

- *Three-line cameras and along-track stereo coverage:* In this case, three linear arrays are used to capture backward-looking, nadir, and forward-looking scenes, as demonstrated in Fig. 3(c). Continuous stereo or triple coverage can be achieved along the flight line with reduced time gap. However, different radiometric qualities exist among the captured scenes. This method is implemented in MOMS and ADS40 [10], [11].

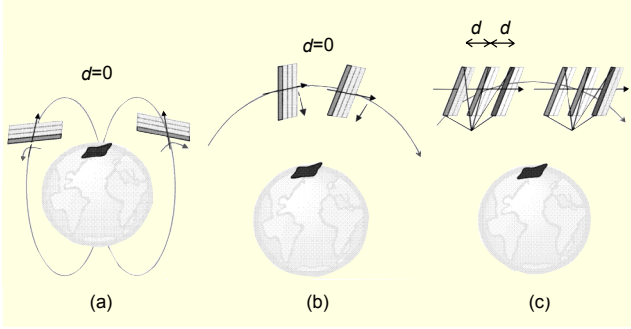


Fig. 3. Three scenarios showing the attainment of stereo coverage in line cameras by using (a) roll angles in two flight lines, (b) pitch angles in the same flight line, and (c) a three-line camera in the same flight line.

IV. Epipolar Geometry of Line Camera Scenes

As mentioned earlier in the introduction, Kim [4] investigated the epipolar geometry of scenes captured by line cameras moving in a trajectory, where the position and heading components are described by second-order polynomial functions and the roll and pitch angles are represented by first-order polynomials. The author concluded that the epipolar lines in scenes captured from such a trajectory are not straight lines. In this research, we will be investigating the epipolar geometry of line cameras moving along their trajectory with constant velocity and attitude. Such a flight path is a subclass of the one investigated by Kim [4]. The main objective of this investigation is to see whether such a simplification would lead to straight epipolar lines. Before going into the details of the epipolar geometry for such a trajectory, we will outline one principle that distinguishes the epipolar geometry of line cameras from that associated with frame cameras.

The main characteristic of scenes captured by line cameras is the fact that each individual image in the scene has its own perspective center. This nature will affect the epipolar geometry in line cameras as follows: for a given point in the left scene, there will be *multiple epipolar planes* in the right scene. Hence, the epipolar line cannot be simply defined as the intersection of two distinct planes as for frame cameras. To illustrate this issue, Fig. 4 shows a schematic drawing of two scenes captured by a line camera. In this figure, one can see that for a given image, point p in the left scene with O as the corresponding perspective center, there will be several epipolar planes. More specifically, there will be as many epipolar planes as the number of involved images/perspective centers in the right scene. In this case, the epipolar line will be defined as the intersection of several epipolar planes with the corresponding image lines (i.e., the epipolar plane and the image line sharing the same perspective center). Therefore, one should expect that the nature of the change in the exterior orientation parameters

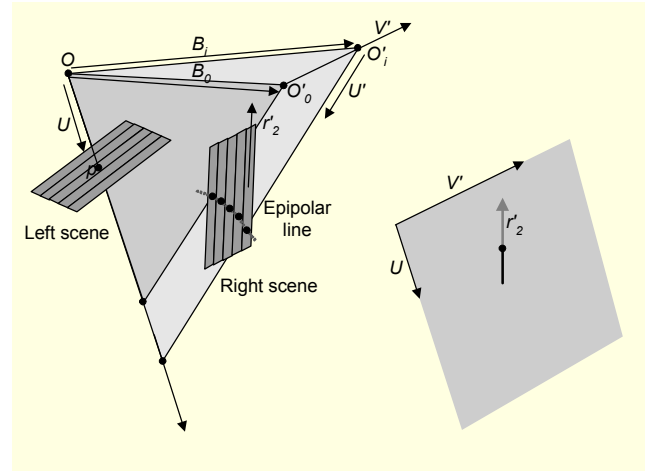


Fig. 4. Non-straightness of epipolar lines in scenes captured by a line camera due to the non-coplanarity of vectors (V', U, r_2) .

during the scene capture will affect the shape of the resulting epipolar line.

1. Epipolar Geometry for Constant Velocity and Attitude Trajectory

The motivation of investigating the constant velocity and attitude trajectory is that satellite scenes are usually acquired in very short time intervals (e.g., about one second for an IKONOS scene). Therefore, the line camera can be assumed to travel with constant velocity and attitude during the scene capture. Another motivation for investigating this trajectory is to test whether it will lead to straight epipolar lines.

Figure 4 shows two scenes captured by a line camera, where the right epipolar line corresponding to the left scene point p is sought. As discussed in frame cameras, the epipolar line can be determined using the coplanarity condition in (1). The major difference between frame and line cameras is the fact that the air base vector will change as the line camera moves along its trajectory. For a line camera moving with a constant velocity, the air base vector associated with a specific scan line/image i , B_i , can be expressed as

$$B_i = \begin{bmatrix} B_{xi} \\ B_{yi} \\ B_{zi} \end{bmatrix} = \begin{bmatrix} X'_{0i} - X_0 \\ Y'_{0i} - Y_0 \\ Z'_{0i} - Z_0 \end{bmatrix} = \begin{bmatrix} X'_0 + V'_x i - X_0 \\ Y'_0 + V'_y i - Y_0 \\ Z'_0 + V'_z i - Z_0 \end{bmatrix} = \begin{bmatrix} B_{x0} + V'_x i \\ B_{y0} + V'_y i \\ B_{z0} + V'_z i \end{bmatrix}, \quad (2)$$

where X_0, Y_0, Z_0 are the coordinates of the perspective center of the image containing the point of interest in the left scene; $X'_{0i}, Y'_{0i}, Z'_{0i}$ are the coordinates of the perspective center associated with image i in the right scene; X'_0, Y'_0, Z'_0 are the coordinates of the perspective center that corresponds to the

first image in the right scene; V'_X, V'_Y, V'_Z are the components of the velocity vector of the right camera's trajectory; and $B_{X_0}, B_{Y_0}, B_{Z_0}$ are the components of the initial air base vector corresponding to the first image in the right scene.

For a given point in the left scene, the components of vector U will be constant. On the other hand, the components of vector U' in the right scene will depend on the change in the camera's attitude from one scan line to the next. However, for a constant attitude trajectory, this will not be a factor. This vector will be defined as

$$\begin{bmatrix} U'_X \\ U'_Y \\ U'_Z \end{bmatrix} = R' \begin{bmatrix} d \\ y_i \\ -c \end{bmatrix} = \begin{bmatrix} r'_{11}d + r'_{12}y_i - r'_{13}c \\ r'_{21}d + r'_{22}y_i - r'_{23}c \\ r'_{31}d + r'_{32}y_i - r'_{33}c \end{bmatrix}, \quad (3)$$

where d is the distance of the linear array from the principal point, as seen in Figs. 2 and 3; y_i is the coordinate along image i in the right scene, shown in Fig. 2; and r'_{11} to r'_{33} are the elements of the rotation matrix between the image and the object space coordinate systems.

To derive the epipolar line equation, one can substitute (2) and (3) in (1), resulting in (4).

$$\begin{vmatrix} B_{X_0} + V'_X i & B_{Y_0} + V'_Y i & B_{Z_0} + V'_Z i \\ U_X & U_Y & U_Z \\ r'_{11}d + r'_{12}y_i - r'_{13}c & r'_{21}d + r'_{22}y_i - r'_{23}c & r'_{31}d + r'_{32}y_i - r'_{33}c \end{vmatrix} = 0 \quad (4)$$

Using the determinant identity in (5), one can derive the equation of the resulting epipolar line by expanding the determinant in (4), which leads to (6):

$$\begin{vmatrix} a+b & c+d & e+f \\ g & h & i \\ j & k & l \end{vmatrix} = \begin{vmatrix} a & c & e \\ g & h & i \\ j & k & l \end{vmatrix} + \begin{vmatrix} b & d & f \\ g & h & i \\ j & k & l \end{vmatrix}, \quad (5)$$

$$E_1 y_i + E_2 i y_i + E_3 i + E_4 = 0, \quad (6)$$

where

$$E_1 = \begin{vmatrix} B_{X_0} & B_{Y_0} & B_{Z_0} \\ U_X & U_Y & U_Z \\ r'_{12} & r'_{22} & r'_{32} \end{vmatrix},$$

$$E_2 = \begin{vmatrix} V'_X & V'_Y & V'_Z \\ U_X & U_Y & U_Z \\ r'_{12} & r'_{22} & r'_{32} \end{vmatrix},$$

$$E_3 = -c \begin{vmatrix} V'_X & V'_Y & V'_Z \\ U_X & U_Y & U_Z \\ r'_{13} & r'_{23} & r'_{33} \end{vmatrix} + d \begin{vmatrix} V'_X & V'_Y & V'_Z \\ U_X & U_Y & U_Z \\ r'_{11} & r'_{21} & r'_{31} \end{vmatrix}, \text{ and}$$

$$E_4 = -c \begin{vmatrix} B_{X_0} & B_{Y_0} & B_{Z_0} \\ U_X & U_Y & U_Z \\ r'_{13} & r'_{23} & r'_{33} \end{vmatrix} + d \begin{vmatrix} B_{X_0} & B_{Y_0} & B_{Z_0} \\ U_X & U_Y & U_Z \\ r'_{11} & r'_{21} & r'_{31} \end{vmatrix}.$$

It can be seen that the relationship between the scene coordinates (i, y_i) in (6) does not represent a straight line due to the presence of the E_2 term. This finding should come as no surprise since the scene coordinates (i, y_i) are involved in two rows of the determinant in (4) (first and third rows, respectively). This can be contrasted to the determinant associated with frame cameras, where the scene/image coordinates are confined to the third row in (1). It is worth mentioning that Gupta and Hartley [12] derived a similar equation for the epipolar lines. They proved that epipolar lines are shaped like a hyperbola, where only one of the two branches is visible in the scene. Equation (6) provides a re-interpretation of Gupta and Hartley's equation where the physical meaning of the involved terms is presented. The remainder of this paper will investigate the factors that will affect the amount of deviations in the derived epipolar lines from being straight. In addition, special imaging configurations resulting in straight epipolar lines will be presented.

A closer look at the E_2 term reveals that it describes the triple products of vectors (V', U, r'_2) as shown in Fig. 4. The r'_2 vector is the second column of the rotation matrix R' . This column represents the components of the unit vector along the scan line direction $(0, 1, 0)^T$ relative to the ground coordinate system. It can be seen that these three vectors will never be coplanar

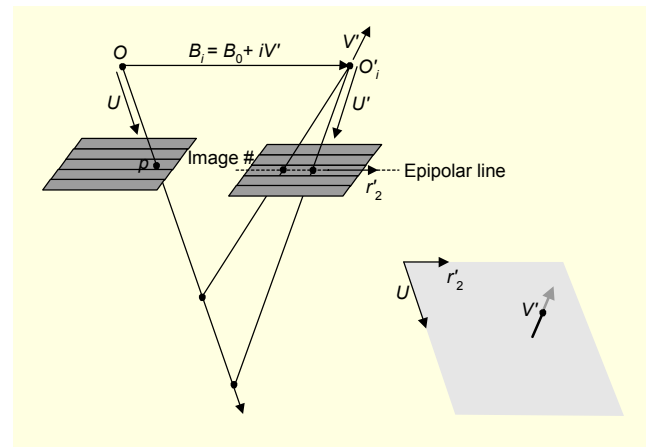


Fig. 5. Straightness of epipolar lines in ideal across-track stereo coverage configuration due to the coplanarity of vectors (B_i, U, r'_2) .

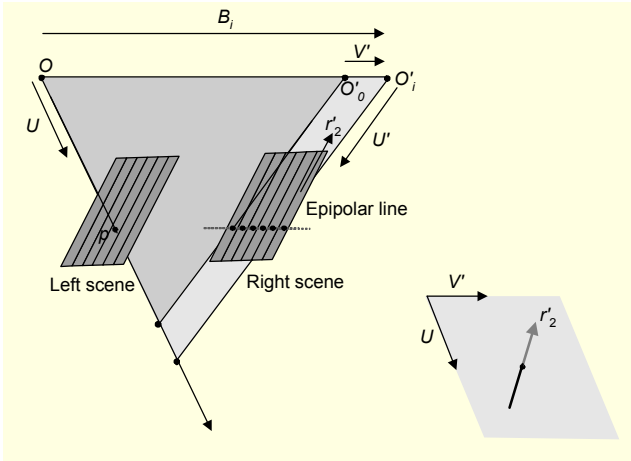


Fig. 6. Straightness of epipolar lines in ideal along-track stereo coverage configuration due to the collinearity of vectors (B_i, V') .

regardless of the stereo coverage configuration, as shown in Figs. 5 and 6. Therefore, the epipolar line will not be straight.

2. Special Cases for Straight Epipolar Lines in Scenes Captured by Line Cameras

There are some special cases that would lead to straight epipolar lines. These special cases will be denoted as the ideal across-track and ideal along-track stereo configurations as seen in Figs. 5 and 6, respectively. For the ideal across-track stereo configuration, the three vectors (B_i, U, r'_2) are coplanar as shown in Fig. 5. Therefore, the epipolar lines will coincide with the scene rows (i.e., they will become straight lines). Ideal along-track stereo configuration requires the collinearity of the velocity and air base vectors, as shown in Fig. 6. Therefore, all epipolar planes (formed by the point of interest in the left scene, its perspective center, and the perspective centers of the right scene) will coincide, forming a unique epipolar plane. Thus, the intersection of such a plane with the scene plane results in a straight epipolar line. The previous requirements for having straight epipolar lines in along-track and across-track stereo configurations can be verified using (6) as follows.

Ideal along-track stereo configuration: This configuration requires the collinearity of the initial air base and velocity vectors (i.e., $B_o = \lambda i V'$, where λ is a scale factor). In this case, the determinants in (6) will be related to each other as

$$\begin{aligned} E_1 &= \lambda E_2, \\ E_4 &= \lambda E_3. \end{aligned} \quad (7)$$

Thus, the locus of the epipolar line, (6), can be rewritten and reduced to

$$\begin{aligned} \lambda E_2 y_i + E_2 i y_i + E_3 i + \lambda E_3 &= 0, \\ E_2 (\lambda + i) y_i + E_3 (i + \lambda) &= 0, \\ (\lambda + i)(E_2 y_i + E_3) &= 0. \end{aligned} \quad (8)$$

Since $(\lambda + i)$ does not equal zero, the final equation of the epipolar line is defined by (9), which is a straight line.

$$E_2 y_i + E_3 = 0. \quad (9)$$

Ideal across-track stereo configuration: This configuration requires the coplanarity of the air base vector and the left and right linear arrays at a given epoch. From Fig. 5, it can be seen that such a requirement would lead to the coplanarity of the three vectors (B_i, U, r'_2) . Thus, the triple product in (10) is reduced to zero.

$$\begin{vmatrix} B_{x_o} + V'_x i & B_{y_o} + V'_y i & B_{z_o} + V'_z i \\ U_x & U_y & U_z \\ r'_{12} & r'_{22} & r'_{32} \end{vmatrix} = 0. \quad (10)$$

Using the identity in (5), the determinant in (10) is equivalent to $(E_1 + E_2 i)$. Consequently, (6) reduces to the straight epipolar line described by

$$E_3 i + E_4 = 0. \quad (11)$$

In summary, in the general case of a line camera moving with constant velocity and attitude along its trajectory, the resulting epipolar lines will not be straight. However, for some special cases, the epipolar lines will be straight. For across-track stereo coverage situations where the left vector U , the right linear array, and the corresponding air base are coplanar, the resulting epipolar lines will be straight. In such a case, the epipolar lines will coincide with the scene rows as in (11). For along-track stereo coverage situations where the air base and velocity vectors are collinear, the epipolar lines will be straight and aligned along the scene columns as in (9). These ideal cases can be rarely realized in practice. Therefore, the remainder of this paper will be dedicated to analyzing the deviation from straightness of the epipolar lines beyond these ideal situations. In the next section, the non-straightness will be quantified by the maximum deviation within the resulting epipolar line from the straight line connecting the end points of that epipolar line.

V. Experimental Result

Several experiments have been conducted in this research.

Table 1. Experiments configuration and layout.

Stereo observation	Roll	Pitch	Heading	AFOV			
				0.93°	10.17°	19.28°	28.15°
Along-track (pitch)	0°	26°	5.0°	Exp.1	Exp.2	Exp.3	Exp.4
Along-track (three-line)	0°	0°	5.0°	Exp.5	Exp.6	Exp.7	Exp.8
Across-track	26°	0°	5.0°	Exp.9	Exp.10	Exp.11	Exp.12
Along-track (pitch)	0°	26°	0.25°	Exp.13	Exp.14	Exp.15	Exp.16
Along-track (three-line)	0°	0°	0.25°	Exp.17	Exp.18	Exp.19	Exp.20
Across-track	26°	0°	0.25°	Exp.21	Exp.22	Exp.23	Exp.24

The objectives of these experiments can be summarized as follows:

- Investigate the non-straightness of the resulting epipolar lines from different stereo-coverage imaging configurations; namely, across-track and along-track stereo coverage.
- Investigate the impact of the amount of deviation from the ideal along-track and ideal across-track stereo configurations on the non-straightness of the resulting epipolar lines.
- Investigate the non-straightness of the resulting epipolar lines from imaging systems with different angular field of views (AFOV).

In these experiments, the non-straightness is quantitatively evaluated by determining the maximum deviation along the epipolar line from the straight line defined by the end points of that epipolar line. We simulated several stereo-scenes to resemble across-track and along-track stereo coverage, as shown in Fig. 7. The departure from the ideal situations has been realized by changing the heading angles between the two scenes constituting the stereo-pair. A total of twenty-four experiments

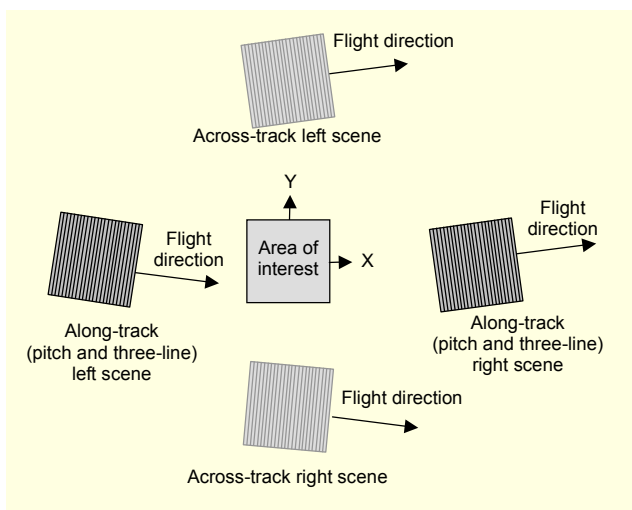


Fig. 7. Layout of along-track and across-track stereo coverage.

were tested and are represented by the shaded cells in Table 1. The principal distance of the imaging system has been changed to produce varying AFOVs in the range from 0.93° to 28.15°. In each of these experiments, three points are selected along the scan line in the left scene, as shown in Fig. 8(a). The epipolar lines were determined and plotted according to (6). Figures 8(b), 8(c), and 8(d) show the epipolar lines for experiments 4, 8, and 12, respectively. In these figures, the point with the maximum deviation from the straight line connecting the end points of the resulting epipolar line is annotated with a circle. The plots in Fig. 9 show the maximum deviation value against the angular field of view for the various experiments in Table 1.

A closer look at the above figures reveals the following facts:

- Along-track stereo coverage by changing the pitch angles and using three-line cameras produces epipolar lines with identical behavior, as can be seen in Fig. 9. This should be expected since these scenes have identical imaging geometry.
- Along-track stereo coverage produces epipolar lines that are closer to being straight than those resulting in across-track stereo coverage.
- As the stereo coverage configuration gets closer to the ideal cases (zero-heading change), the resulting epipolar lines become closer to being straight, as indicated by a smaller maximum deviation. This can be seen by comparing the plots in Figs. 9(a) and 9(b), where the deviation from the ideal cases is implemented through the heading changes of 5° and 0.25°, respectively.
- Finally, as the angular field of view decreases, the epipolar lines become straighter. As mentioned earlier, the angular field of view has been decreased by increasing the principal distance while maintaining the same size of the scan line.

The previous analysis allowed us to investigate the influence of the imaging system's specification and trajectory on the shape of the resulting epipolar lines. Such an analysis is important for epipolar resampling since the resampling process aims at transforming the original scenes in such a way that the

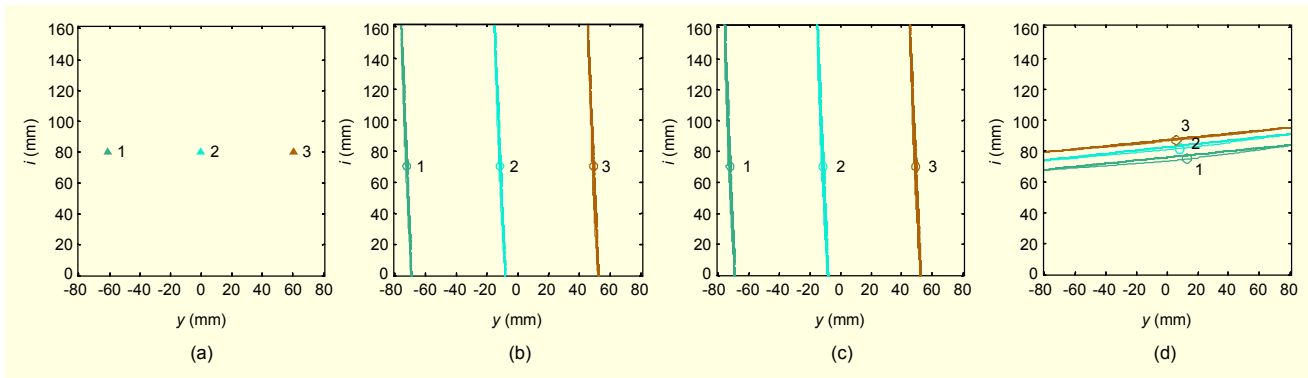


Fig. 8. Three points selected in (a) the left scene, whose epipolar lines in the right scene are sought and analyzed in experiments (b) 4, (c) 8, and (d) 12.

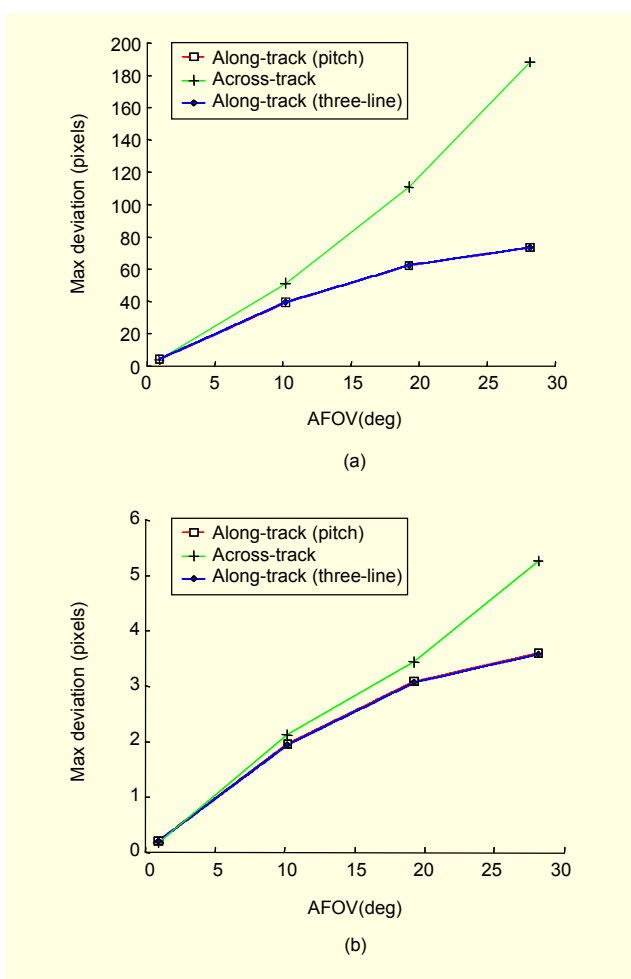


Fig. 9. The relationship between the maximum deviation from the straightness of the epipolar lines and the AFOV for headings (a) 5° and (b) 0.25°.

epipolar lines coincide with the rows or columns of the normalized scene. Therefore, for line cameras, transforming non-straight epipolar lines into straight lines in the final normalized scenes will introduce some distortion. The amount

of this distortion will increase as the deviations of the original epipolar lines from being straight increase. Therefore, it was important to investigate the factors that affect such deviations.

VI. Conclusions and Recommendations for Future Work

This paper outlined a comprehensive investigation of the epipolar geometry of line cameras moving with constant velocity and attitude. It has been shown that the epipolar geometry for such cameras is far more complicated than that of frame images. The epipolar line equation has been developed. This equation turned out to represent non-straight epipolar lines. However, there are two special cases that would yield straight epipolar lines. First, across-track stereo coverage yields straight epipolar lines whenever the air base vector at some epoch is coplanar with the linear arrays at the same epoch. In such a case, the epipolar lines coincide with the scene rows. Second, along-track stereo coverage yields straight epipolar lines whenever the air base and the velocity vector of the right scene are collinear. In this case, for a given point in the left scene, a unique epipolar plane will be defined across the right scene. However, such scenarios are rarely achieved in practice.

The paper proceeded by analyzing the deviation from straightness in the resulting epipolar lines from imaging situations beyond those ideal cases. This analysis is motivated by the fact that normalized image generation aims at manipulating the original scenes in such a way that the epipolar lines are transferred to coincide with corresponding rows or columns. Thus, having non-straight epipolar lines would yield distortions in the normalized images. Therefore, it is important to investigate the factors that influence the deviation from straightness. It has been established that along-track stereo coverage yields epipolar lines that are closer to being straight when compared to those associated with across-track stereo coverage. Moreover, as the camera's angular field of view decreases, the epipolar lines become straighter. Therefore, one

should expect that the epipolar geometry is easier to establish for space-borne imagery than airborne imagery. This is due to the fact that the former imagery has a smaller angular field of view. Scenes with zero angular field of view represent an extreme case, which would yield straight epipolar lines. This would be the case as the camera's principal distance approaches infinity. It should be noted that for such scenes the imaging geometry is represented by a parallel rather than perspective projection. Therefore, future research will focus on investigating the epipolar geometry of scenes captured according to parallel projection. Moreover, the influence of the departure from parallel projection on the epipolar geometry will be investigated and evaluated.

References

- [1] Y. Wang, "Automated Triangulation of Linear Scanner Imagery," *Joint Workshop of ISPRS WG I/1, I/3 and IV/4 on Sensors and Mapping from Space*, Hannover, 1999.
- [2] L. Fritz, "Recent Developments for Optical Earth Observation in the United States," *Photogrammetric Week*, Stuttgart, 1995, pp.75-84.
- [3] W. Cho, T. Schenk, and M. Madani, "Resampling Digital Imagery to Epipolar Geometry," *Int'l Archives of Photogrammetry and Remote Sensing*, 29(B3), Washington DC, USA, 1992, pp.404-408.
- [4] T. Kim, "A Study on the Epipolarity of Linear Pushbroom Images," *J. of Photogrammetric Eng. & Remote Sensing*, vol. 66, no. 8, 2000, pp. 961-966.
- [5] T. Schenk, *Digital Photogrammetry - Volume I*, TerraScience, Laurelville, Ohio, USA, 1999, p.428.
- [6] K. Kraus, *Photogrammetry*, vol. 1, Dümmler Verlag, Bonn., 1993, p. 397.
- [7] A. Habib and B. Beshah, "Modeling Panoramic Linear Array Scanner," *ISPRS Commission III Symposium*, Columbus, Ohio, 6 - 10 July, 1998.
- [8] H. Sohn, H. Yoo, and S. Kim, "Evaluation of Geometric Modeling for KOMPSAT-1 EOC Imagery Using Ephemeris Data," *ETRI J.*, vol. 26, no. 3, June 2004, pp.218-228.
- [9] C. Fraser, H. Hanley, and T. Yamakawa, "Sub-Metre Geopositioning with IKONOS GEO Imagery," *ISPRS Joint Workshop on High Resolution Mapping from Space*, Hannover, Germany, 2001.
- [10] C. Heipke, W. Kornus, and A. Pfannenstien, "The Evaluation of MEOSS Airborne Three-Line Scanner Imagery: Processing Chain and Results," *J. of Photogrammetric Eng. & Remote Sensing*, vol. 62, no. 3, 1996, pp. 293-299.
- [11] R. Sandau, B. Braunecker, H. Driescher, A. Eckardt, S. Hilbert, J. Hutton, W. Kirchhofer, E. Lithopoulos, R. Reulke, and S. Wicki, "Design Principles of the LH Systems ADS40 Airborne Digital Sensor," *Int'l Archives of Photogrammetry and Remote Sensing*, 33(B1), Amsterdam, Netherlands, 2000, pp. 258-265.
- [12] R. Gupta and R. I. Hartley, "Linear Pushbroom Cameras," *IEEE Trans. on Pattern Analysis and Machine Intelligence*, vol. 19, no. 9, 1997, pp. 963-975.



Ayman F. Habib received the MSc in civil engineering from Cairo University, Egypt, and the MSc and PhD in photogrammetry from the Ohio State University, USA. Currently, he is an Associate Professor at the Department of Geomatics Engineering, University of Calgary, Canada. His research interests span the fields of terrestrial and aerial mobile mapping systems, modeling the perspective geometry of imaging scanners, automatic matching and change detection, incorporation of linear features in various orientation procedures, object recognition in imagery, and integration of photogrammetric data with other sensors/datasets.



Michel F. Morgan received the MSc in geographic information systems from the International Institute for Aerospace Survey and Earth Sciences, The Netherlands, the MSc in geodetic science from the Ohio State University, USA, and the PhD in photogrammetry from the University of Calgary, Canada. Currently, he is a post doctoral fellow at the Department of Geomatics Engineering, University of Calgary, Canada. His research interests focus on modeling the perspective geometry of line cameras.



Soo Jeong received the BS, MSc, and PhD degrees in civil engineering from Yonsei University in 1988, 1990, and 1997. He was with Korea Aerospace Research Institute (KARI) in Daejeon, Korea from 2000 to 2001. He was with Electronics and Telecommunications Research Institute (ETRI) in Daejeon, Korea, from 2001 to 2005. He is now in a faculty position in the Department of Civil Engineering, Andong National University, Korea. He is interested in software development for photogrammetric work.



Kyung-Ok Kim received the MSc degree in computer science from Ohio State University, and PhD degree in computer engineering from Chungnam National University in Korea. She has worked for ETRI in Korea from 1988 to 2005. She is interested in processing multi-sensor data fusion for hyperspectral, Lidar, SAR, and high resolution optical imagery.